J Toxicol Pathol 2015; 28: 21–26

Original Article

Establishment of a syngeneic orthotopic model of prostate cancer in immunocompetent rats

Shugo Suzuki[1, 2], Aya Naiki-Ito[1], Toshiya Kuno[1], Wanisa Punfa[1, 3], Ne Long[4], Hiroyuki Kato[1], Shingo Inaguma[1, 5], Masami Komiya[1, 6], Tomoyuki Shirai[1, 7], and Satoru Takahashi[1,*]

[1] Department of Experimental Pathology and Tumor Biology, Nagoya City University Graduate School of Medical Sciences, 1 Kawasumi, Mizuho-cho, Mizuho-ku, Nagoya, Aichi 467-8601, Japan
[2] Pathology Division, Nagoya City East Medical Center, 1-2-23 Wakamizu, Chikusa-ku, Nagoya, Aichi 464-8547, Japan
[3] Department of Biochemistry, Faculty of Medicine, Chiang Mai University, Chiang Mai, 50200, Thailand
[4] National Center for Geriatrics and Gerontology, 35 Gengo, Morioka-machi, Obu, Aichi, 474-8511, Japan
[5] Department of Pathology, Aichi Medical University School of Medicine, 1-1 Yazakokarimata, Nagakute, Aichi 480-1195, Japan
[6] Division of Cancer Prevention Research, National Cancer Center Research Institute, 5-1-1 Tsukiji, Chuo-ku, Tokyo 104-0045, Japan
[7] Nagoya City Rehabilitation Center, 1-2 Mikanyama, Yatomi-cho, Mizuho-ku, Nagoya, Aichi 467-0036, Japan

Abstract: We previously established 3 cell lines (PLS10, PLS20 and PLS30) from a chemically-induced prostate carcinoma in F344 rats, and demonstrated high potential for metastasis in nude mice. In the present study, we investigated the feasibility of establishing an orthotopic model using the 3 rat prostate cancer cell lines in immunocompetent rats with the aim of resolving species-mismatch problems and defects of immune systems. The PLS10, PLS20 and PLS30 cell lines were injected into the ventral prostates of 6-week-old rats, which were then sacrificed at experimental weeks 4 and 8. Tumor mass formation was found in rats with PLS10, but not in those with PLS20 or PLS30. Additionally, metastatic carcinomas could be detected in lymph nodes and lungs of PLS10-inoculated rats. Genetic analysis demonstrated K-ras gene mutations in PLS10 and PLS20, but not in PLS30 cells. There were no mutations in p53 and KLF6. In conclusion, we established a syngeneic orthotopic model for prostate cancer in immunocompetent rats simulating human castration-resistant prostate cancer (CRPC), which should prove useful for development and validation of therapeutic agents, especially with immunotherapy. (DOI: 10.1293/tox.2014-0050; J Toxicol Pathol 2015; 28: 21–26)

Key words: orthotopic model, prostate cancer, rats, immunocompetent animal

Introduction

Prostate cancer is the second most frequently diagnosed cancer in males in the world, with especially high incidences in Oceania, Europe and North America[1, 2]. Recently, the occurrence of prostate cancer has been increasing in Japan[3]. Androgen ablation therapy is a widely used treatment during the initial stage of the disease that may produce an initially favorable outcome, but many patients eventually develop castration-resistant prostate cancer (CRPC) with metastatic foci, which cause patient death[2]. Therefore, understanding of the mechanisms of the acquisition of metastatic potential and the castration-resistant phenotype of cancer cells is urgently required.

Previously, we developed a CRPC model with a 3,2'-dimethyl-4-aminobiphenyl plus testosterone treatment in F344 rats[4]. Cancer in this model features scirrhous growth with abundant collagenous tissue and inflammatory infiltration. To facilitate molecular analyses, we established cancer cell lines, PLS10, PLS20 and PLS30, from this CRPC model[5]. All of these cell lines formed tumor masses and lung metastases in nude mice when implanted subcutaneously. Moreover, androgen receptor (AR) expression in the 3 cell lines was found to be downregulated due to hypermethylation in the AR promoter region[6], so they can be utilized to determine the mechanisms of progression and/or development of new drugs for prostate cancer *in vitro*, and *in vivo* with nude mice[7, 8]. In the present study, we investigated establishment of a syngeneic orthotopic prostate cancer model using PLS10, PLS20 or PLS30 cells in immunocompetent rats to create feasible conditions for anticancer drug development in a species-matched tumor microenvironment. To further investigate the differences of cell lines, we employed SSCP-PCR for detection of gene mutations in K-ras, p53 and a tumor suppressor gene for prostate cancer, KLF6[9].

Received: 28 October 2014, Accepted: 18 November 2014
Published online in J-STAGE: 18 December 2014
*Corresponding author: S Takahashi
(e-mail: sattak@med.nagoya-cu.ac.jp)

Materials and Methods

Cell culture

The PLS10, PLS20 and PLS30 cell lines were cultured in Roswell Park Memorial Institute-1640 Medium (RPMI 1640, Gibco, Carlsbad, CA, USA) with 10% fetal bovine serum (FBS), 50 U/ml penicillin and 50 μg/ml streptomycin in a humidified incubator with an atmosphere comprising 95% air and 5% CO_2 at 37°C.

Animals

All animal experiments were performed under protocols approved by the Institutional Animal Care and Use Committee of Nagoya City University Graduate School of Medical Sciences. Five-week-old male F344 rats were purchased from Charles River Laboratories Japan Inc. (Atsugi, Japan) and housed in plastic cages with hardwood chip bedding in an air-conditioned room at 23 ± 2°C and 55 ± 5% humidity with a 12 hr light/dark cycle. Oriental MF powder diet (Oriental Yeast Co., Ltd., Tokyo, Japan) and distilled water were available *ad libitum*.

Orthotopic xenograft model with prostate cancer cell lines

After one week of acclimation, rats were divided into 3 groups of 12 or 13 animals each. PLS10, PLS20 or PLS30 cells (5×10^6) were mixed with 50% Matrigel (BD Biosciences) and injected (50 μL) into the ventral prostate of each rat. At sacrifice at experimental weeks 4 and 8, the liver, lung, kidneys and lymph nodes and primary tumors in the prostate were removed and fixed in 10% buffered formalin. At least 1 section of each tissue and the largest section from each lobe of the lung were processed for hematoxylin and eosin (H&E) staining. To determine variation in tumorigenesis with inoculated cell number, PLS10 (2 or 5×10^6) cells were injected into the ventral prostate. Rats were sacrificed at experimental week 8, and then primary tumors in the prostate and the same organs as mentioned above were removed and fixed in 10% buffered formalin. Primary tumors were measured and tumor volume was calculated using the following formula: tumor volume = $(\text{width})^2$ x length/2.

PCR-SSCP analysis of K-ras, p53 and KLF6

Exons 1 and 2 of K-ras, exons 2 to 10 of p53, and exons 1 to 4 of KLF6 were analyzed by the PCR-SSCP method as previously reported[10, 11]. The primers are listed in Table 1. If shifted bands were observed in the PCR-SSCP analysis, they were cut from the acrylamide gel to be sequenced (ABI PRISM® 310 Genetic Analyzer; Life Technologies Corporation, Carlsbad, CA, USA).

Statistical analysis

Statistical analyses were performed with mean ± SD values using one-way ANOVA, Bonferroni correction or the Dunnett's test. Statistical significance was concluded at $P< 0.05$, $P<0.01$ or $P<0.001$.

Table 1. The Sequences of the Primers Used for PCR-SSCP analysis and Direct Sequencing

Gene		Sequence
K-ras	exon 1	5'-TTATTATAAGGCCTGCTGAA-3'
		5'-CATAGAATATAAAGCAGCAT-3'
	exon 2	5'-CAGGACTCCTACAGGAAACA-3'
		5'-AAACCCACCTATAATGGTGA-3'
P53	exon 2	5'-TGCATCCATACAGTACACAG-3'
		5'-AGGGGCCCTGTAAGATCCAC-3'
	exon 3	5'-GGAACTAATTCTCTGCTCTT-3'
		5'-GTCCCCTCTTGCCCGGCTCC-3'
	exon 4 A	5'-GGTCTTCTTTGGCCCATCC-3'
		5'-CCACGGTGTAGCTGAAGCAG-3'
	exon 4 B	5'-GCACAGGAACCTGGAACTGA-3'
		5'-GGCATTTAAAGTCAGACGAA-3'
	exon 5	5'-CGCTGACCTTTGATTCTTTC-3'
		5'-TCTAACCCCACAGCAGTGCC-3'
	exon 6	5'-CCGGCCTCTGACTTATTCTT-3'
		5'-ACCTGGCACACAGCTTCCTA-3'
	exon 7	5'-CCTCCTCTTGTCCCGGGTAG-3'
		5'-CTTCTTTGTCCTGCCTGCTC-3'
	exon 8	5'-CAAAGTCACCCTTGCTCTC-3'
		5'-TAATCCAATAATAACCTTGG-3'
	exon 9	5'-CTGTCCTACTTCATCCTTGC-3'
		5'-GGCGCTGCCCCAGGTCACTC-3'
	exon 10	5'-CCTCCCTTTTCTGTATTCCT-3'
		5'-GGGCCGAGTACTATCTACAA-3'
KLF6	exon 1	5'-GGAGACTGTCTTTTCCAACC-3'
		5'-GGCGCACCGGGCAGGTGAAA-3'
	exon 2A	5'-GTCAGTGGCCGTAACAGTCA-3'
		5'-TCTTCAGTTCTGATTCCTCC-3'
	exon 2B	5'-GTGGACCAAAATCATTCTAGCAC-3'
		5'-GGGGTCAGAGGTAAACTT-3'
	exon 2C	5'-CGGAGGAACTTTCGCCCACG-3'
		5'-GTCGCCAGACTTCCCCGAGGTC-3'
	exon 2D	5'-CTCACCTGGGAAGGTTCGAAGT-3'
		5'-CCCACCAGCAGCTGACCG-3'
	exon 3	5'-CAGTGAAGTCATGTGCTCTTG-3'
		5'-ACACTTCTTTTTCATTGACGTA-3'
	exon 4	5'-GAGGACTTGTACAGGGACCG-3'
		5'-AGCCTCTTTTAGCCTACAGGA-3'

Results

Four and eight weeks after inoculation, tumor masses were found in the ventral prostate in nearly all rats with PLS10 (Figs. 1A, B), but not in those with PLS20 or PLS30 (Table 2). The average primary tumor sizes in the PLS10-inoculated rats were 343 ± 247 and 2114 ± 391 mm^3 at 4 and 8 weeks, respectively. At 8 weeks, because of tumor extension around prostate lobes, stricture of the urethra was detected with bladder distension in some PLS10-inoculated rats. On histological assessment, adenocarcinoma elements were found to have spread from the ventral prostate area to the surroundings, with various levels of differentiation (Figs. 1C–E), and to have invaded perineural spaces, and vascular and lymph vessels (Figs. 1F–H) in the PLS10-inoculated rats. Additionally, there were some metastatic carcinomas in lymph nodes and lungs (Figs. 1I, J). Two of 6 rats had lymph node metastasis at week 4, and metastases to lymph nodes and lungs were found in 5 and 3 rats among 6 tumor-bearing

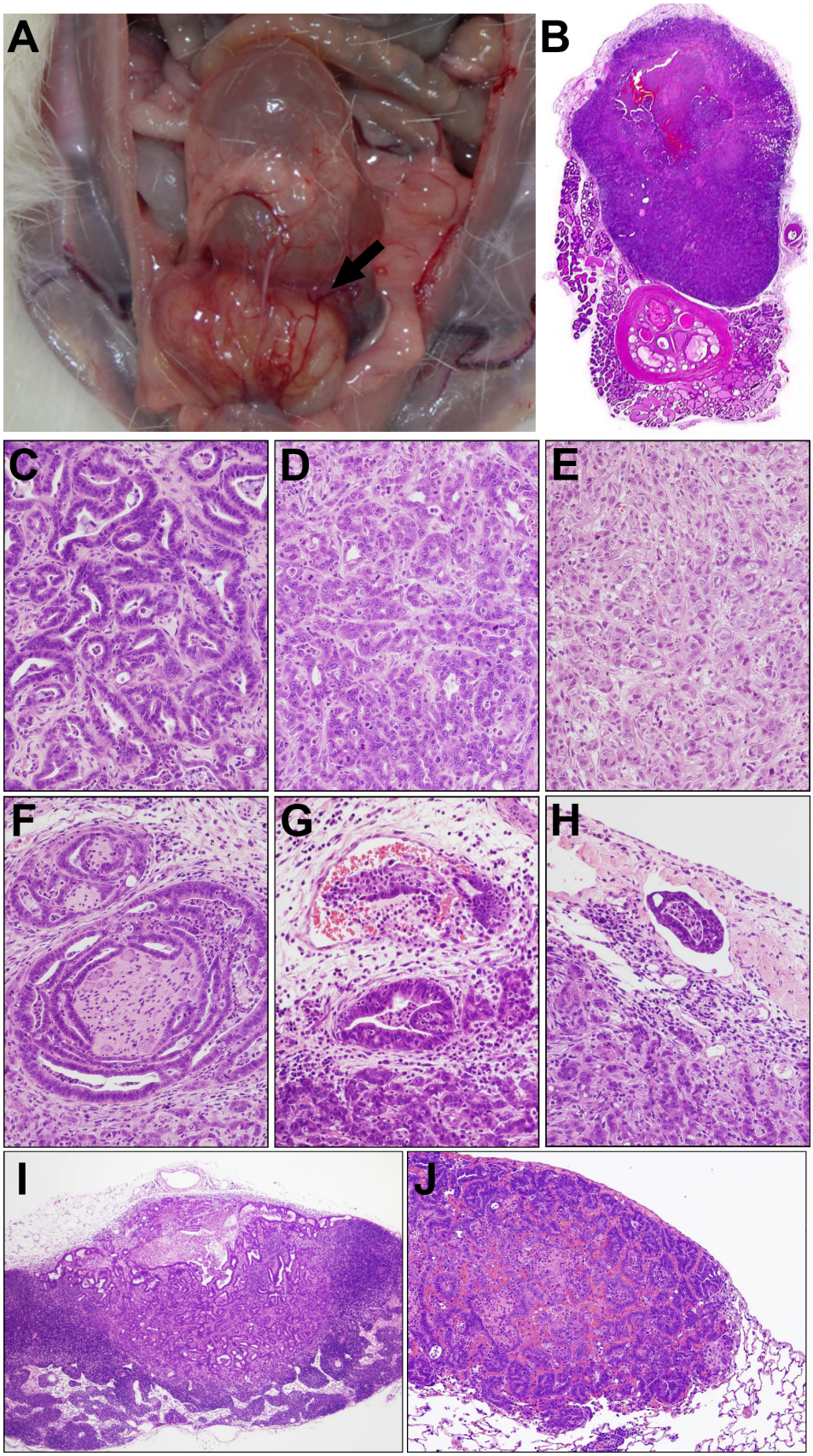

Fig. 1. Macroscopic findings for PLS10 tumors in the ventral prostate of F344 rats at week 8. A large tumor mass is present in the ventral lobe (arrow) (A). Low magnification view of a prostate tumor formed in the ventral lobe at experimental week 4 (B). Tumors consisted of well differentiated (C), moderately differentiated (D) and poorly differentiated (E) components, infiltrating perineural areas (F), invading vascular (G) and lymph vessels (H), and metastasizing to lymph nodes (I) and lungs (J) at experimental week 8.

Table 2. Tumoigenesity and Metastatic Potential of Rat Prostate Cancer Cell Lines in F344 Rats

Cell line	4 weeks					8 weeks				
	No. of rats	Tumori-genicity	Tumor volume (mm^3)	LN metastasis	Lung metastasis	No. of rats	Tumori-genicity	Tumor volume (mm^3)	LN metastasis	Lung metastasis
PLS10	6	6	343 ± 247	2	0	7	6	2114 ± 391	5	3
PLS20	6	0	0 ± 0	0	0	7	0	0 ± 0	0	0
PLS30	6	0	0 ± 0	0	0	6	0	0 ± 0	0	0

LN: Lymph node.

Table 3. Tumoigenesity and Metastatic Potential in Different Cell Number of PLS10 at 8 Weeks

Cell No.	No. of rats	Tumori-genicity	Tumor volume (mm^3)	LN metastasis	Lung metastasis
2×10^6	6	6	3724 ± 1707	2	1
5×10^6	6	5	3745 ± 1381	3	2

LN: Lymph node.

Table 4. Summary of Characteristics in Rat Prostate Cancer Cell Lines

Cell line	PLS10	PLS20	PLS30
Karyotype*	Diploid	Hypertetraploid	Hyperdiploid
K-ras	G13R	Q61L	Wild
p53	Wild	Wild	Wild
KLF6	Wild	Wild	Wild
AR protein*	-	-	-
Tumorigenicity			
Nude mice* (subcutaneous)	+	+	+
F344 rats (orthotopic)	+	-	-
Histology of xenograft*	Wel	Por	Wel

AR: Androgen receptor, Wel: Well differentiated adenocarcinoma, Por: Poorly differentiated adenocarcinoma. *The data previous reported by Nakanishi et al. (1996)[4] was included in the Table.

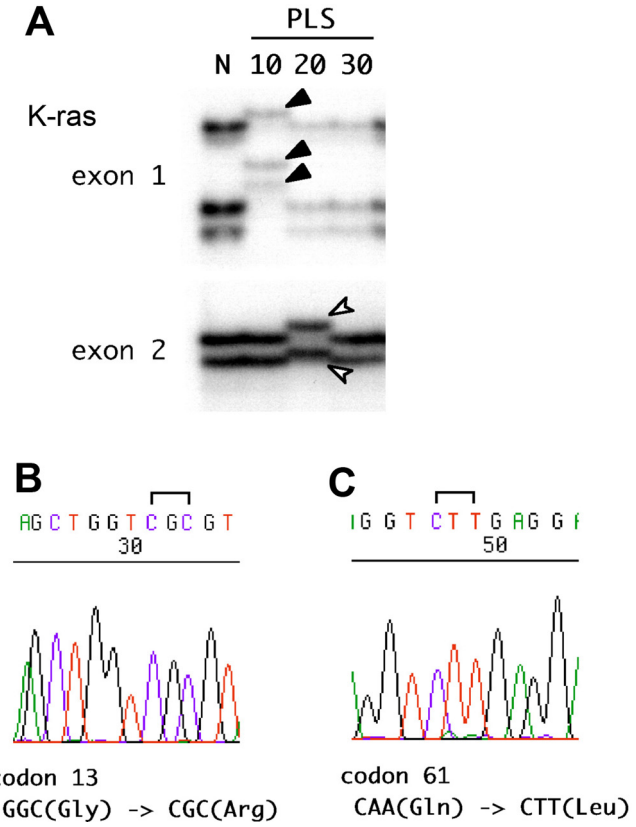

Fig. 2. K-ras gene mutations in cell lines. Aberrant localization of bands was detected in PLS10 at exon 1 and PLS20 at exon 2 of the K-ras gene by SSCP-PCR (A). Mutations of codon 13 (GGC, Gly to CGC, Arg) in PLS10 (B) and codon 61 (CAA, Gln to CTT, Leu) in PLS20 (C) were detected by sequencing.

animals, respectively (Table 2).

In the next experiment, we investigated the effects of different numbers of PLS10 cells. However there were no or very limited differences in tumorigenicity, tumor volume or metastasis to lymph nodes and lungs after 8 weeks (Table 3).

Aberrant localization of bands was detected in PLS10 in exon 1 of the K-ras gene and PLS20 in exon 2 of the K-ras gene (Fig. 2A). After sequencing, mutations of codons 13 (GGC, Gly to CGC, Arg) and 61 (CAA, Gln to CTT, Leu) were detected in PLS10 and PLS20, respectively (Fig. 2B and 2C). There were no mutations of p53 and KLF6 in any of the cell lines (data not shown). Along with findings of a previous report[5], we summarized characteristics of the prostate cancer cell lines, PLS10, PLS20 and PLS30 in Table 4.

Discussion

Treatment with docetaxel has been a standard therapy for CRPC over the last decade, and novel therapeutic options including immunotherapy have recently been developed, however, the prognosis of CRPC is still poor[12, 13]. Therefore, development of new drugs and therapies is absolutely imperative. To date, various immunotherapeutic options for prostate cancer have been developed against cancer-associated antigens such as prostate specific antigen (PSA), prostatic acid phosphatase (PAP), prostate-specific membrane antigen (PSMA), prostate stem cell antigen (PSCA) or cancer/testis antigens[14]. Among them, the US Food and Drug Administration (FDA) approved sipuleucel-T as an immunotherapy for metastatic CRPC to improve overall survival. It is an autologous vaccine using peripheral blood mononuclear cells activated by co-culture with PAP-granulocyte-macrophage colony stimulating factor (GM-

CSF) recombinant fusion protein ex vivo.

For development of drugs and therapeutic approaches, it is also important to develop methods for verification of efficacy. Animal experiments are essential and critical for validation of anti-cancer drugs in preclinical evaluation for bridging the gap between in vitro research data and clinical trials in humans. Several animal models of prostate cancer have been established, including chemical induction of prostate cancer in rodents, implantation of human and rodent tumor cell lines into immunologically compromised animals such as nude mice, and implantation of syngeneic cancers[15, 16]. Many kinds of genetically-engineered mouse model have also been developed in the past 2 decades[17]. However, replication of data from animal studies often fail in clinical trials[18]. To resolve this concern, we should keep in mind that we should carefully choose the animal model most suitable for analysis of stage-specific effects of therapeutic agents. Therefore it is necessary to establish various kinds of experimental systems. We have focused on a series of animal models for various prostate cancer phenotypes: noninvasive and castration-sensitive cancer[19–21], invasive and castration-sensitive cancer[22], invasive and castration-resistant cancer[4] and metastatic and castration-resistant cancer[23] models. In the present study, we developed a syngeneic orthotopic implantation model with metastases in a short period using a prostate cancer cell line, PLS10, in immunocompetent rats.

Accumulating evidence has demonstrated that stromal-epithelial interactions play critical roles in cancer progression[24, 25]. Invasive and androgen-independent carcinomas induced by DMAB and TP within 60 weeks, simulating CRPC in men, is the most appropriate model in the context of tumor microenvironment. However, it has shortcomings in terms of the experimental period necessary for screening a number of drugs. Metastatic and androgen-independent cancer models using nude mice also simulate metastatic CRPC but with a shorter experimental term; however the use of such immunodeficient animals is imperfect in terms of species mismatch between tumor cells and the surrounding stroma and serious defects in immune systems. Considering these points, the syngeneic orthotopic implantation prostate cancer model presented here should prove valuable for analysis of anticancer drug efficacy with a tumor microenvironment resembling the human situation.

The three prostate cancer cell lines derived from rat invasive prostatic carcinoma established in our laboratory have all shown tumorigenicity in nude mice with lung metastases[5]. In the present study, only PLS10 proved tumorigenic in immunocompetent conspecific animals. The results suggest that PLS10 but not PLS20 or PLS30 can escape immune attack from the host. Elucidation of the mechanisms should enable us to discover novel immune recognition targets for killing prostate cancer cells. In the present and previous studies, we detected differences among cell lines (summarized in Table 4), but we have not obtained adequate data about the mechanism of immune escape as yet. More detailed studies are needed for determination of the differences between the PLS10 and PLS20/30 cell lines.

In conclusion, we have established syngeneic orthotopic model of prostate cancer in immunocompetent rats. From an immunological viewpoint, this model will be of practical use for development, screening and validation of therapeutic agents, especially in immunotherapy of metastatic prostate cancer.

Declaration of Conflicting Interests: The authors declare that they have no conflict.

Acknowledgments: This work was supported by a Grant-in-Aid for Cancer Research from the Ministry of Health, Labour and Welfare of Japan and a grant from the Society for Promotion of Pathology of Nagoya, Japan. The authors would like to thank Dr. Malcolm Moore for helpful review of this manuscript.

References

1. Jemal A, Bray F, Center MM, Ferlay J, Ward E, and Forman D. Global cancer statistics. CA Cancer J Clin. **61**: 69–90. 2011. [Medline] [CrossRef]
2. Damber JE, and Aus G. Prostate cancer. Lancet. **371**: 1710–1721. 2008. [Medline] [CrossRef]
3. Matsuda T, Marugame T, Kamo K, Katanoda K, Ajiki W, Sobue T. Japan Cancer Surveillance Research Group Cancer incidence and incidence rates in Japan in 2006: based on data from 15 population-based cancer registries in the monitoring of cancer incidence in Japan (MCIJ) project. Jpn J Clin Oncol. **42**: 139–147. 2012. [Medline] [CrossRef]
4. Shirai T, Tamano S, Kato T, Iwasaki S, Takahashi S, and Ito N. Induction of invasive carcinomas in the accessory sex organs other than the ventral prostate of rats given 3,2′-dimethyl-4-aminobiphenyl and testosterone propionate. Cancer Res. **51**: 1264–1269. 1991. [Medline]
5. Nakanishi H, Takeuchi S, Kato K, Shimizu S, Kobayashi K, Tatematsu M, and Shirai T. Establishment and characterization of three androgen-independent, metastatic carcinoma cell lines from 3,2′-dimethyl-4-aminobiphenyl-induced prostatic tumors in F344 rats. Jpn J Cancer Res. **87**: 1218–1226. 1996. [Medline] [CrossRef]
6. Takahashi S, Inaguma S, Sakakibara M, Cho YM, Suzuki S, Ikeda Y, Cui L, and Shirai T. DNA methylation in the androgen receptor gene promoter region in rat prostate cancers. Prostate. **52**: 82–88. 2002. [Medline] [CrossRef]
7. Pitchakarn P, Ogawa K, Suzuki S, Takahashi S, Asamoto M, Chewonarin T, Limtrakul P, and Shirai T. Momordica charantia leaf extract suppresses rat prostate cancer progression in vitro and in vivo. Cancer Sci. **101**: 2234–2240. 2010. [Medline] [CrossRef]
8. Suzuki S, Pitchakarn P, Sato S, Shirai T, and Takahashi S. Apocynin, an NADPH oxidase inhibitor, suppresses progression of prostate cancer via Rac1 dephosphorylation. Exp Toxicol Pathol. **65**: 1035–1041. 2013. [Medline] [CrossRef]
9. Narla G, Heath KE, Reeves HL, Li D, Giono LE, Kimmelman AC, Glucksman MJ, Narla J, Eng FJ, Chan AM, Ferrari AC, Martignetti JA, and Friedman SL. KLF6, a candidate tumor suppressor gene mutated in prostate cancer. Science. **294**: 2563–2566. 2001. [Medline] [CrossRef]

10. Masui T, Shirai T, Imaida K, Hirose M, Futakuchi M, Tatematsu M, and Ito N. Ki-ras mutations with frequent normal allele loss versus absence of p53 mutations in rat prostate and seminal vesicle carcinomas induced with 3,2′-dimethyl-4-aminobiphenyl. Mol Carcinog. **13**: 21–26. 1995. [Medline] [CrossRef]
11. Masui T, Dong Y, Yamamoto S, Takada N, Nakanishi H, Inada K, Fukushima S, and Tatematsu M. p53 mutations in transitional cell carcinomas of the urinary bladder in rats treated with N-butyl-N-(4-hydroxybutyl)-nitrosamine. Cancer Lett. **105**: 105–112. 1996. [Medline] [CrossRef]
12. Tannock IF, de Wit R, Berry WR, Horti J, Pluzanska A, Chi KN, Oudard S, Théodore C, James ND, Turesson I, Rosenthal MA, Eisenberger MA. TAX 327 Investigators Docetaxel plus prednisone or mitoxantrone plus prednisone for advanced prostate cancer. N Engl J Med. **351**: 1502–1512. 2004. [Medline] [CrossRef]
13. Omlin A, Pezaro C, and Gillessen Sommer S. Sequential use of novel therapeutics in advanced prostate cancer following docetaxel chemotherapy. Ther Adv Urol. **6**: 3–14. 2014. [Medline] [CrossRef]
14. Westdorp H, Sköld AE, Snijer BA, Franik S, Mulder SF, Major PP, Foley R, Gerritsen WR, and de Vries IJ. Immunotherapy for prostate cancer: lessons from responses to tumor-associated antigens. Front Immunol. **5**: 191. 2014. [Medline] [CrossRef]
15. Ahmad I, Sansom OJ, and Leung HY. Advances in mouse models of prostate cancer. Expert Rev Mol Med. **10**: e16. 2008. [Medline] [CrossRef]
16. Lopez-Barcons LA. Human prostate cancer heterotransplants: a review on this experimental model. Asian J Androl. **12**: 509–518. 2010. [Medline] [CrossRef]
17. Wu X, Gong S, Roy-Burman P, Lee P, and Culig Z. Current mouse and cell models in prostate cancer research. Endocr Relat Cancer. **20**: R155–R170. 2013. [Medline] [CrossRef]
18. Begley CG, and Ellis LM. Drug development: Raise standards for preclinical cancer research. Nature. **483**: 531–533. 2012. [Medline] [CrossRef]
19. Shirai T, Fukushima S, Ikawa E, Tagawa Y, and Ito N. Induction of prostate carcinoma in situ at high incidence in F344 rats by a combination of 3,2′-dimethyl-4-aminobiphenyl and ethinyl estradiol. Cancer Res. **46**: 6423–6426. 1986. [Medline]
20. Shirai T, Cui L, Takahashi S, Futakuchi M, Asamoto M, Kato K, and Ito N. Carcinogenicity of 2-amino-1-methyl-6-phenylimidazo [4,5-b]pyridine (PhIP) in the rat prostate and induction of invasive carcinomas by subsequent treatment with testosterone propionate. Cancer Lett. **143**: 217–221. 1999. [Medline] [CrossRef]
21. Asamoto M, Hokaiwado N, Cho YM, Takahashi S, Ikeda Y, Imaida K, and Shirai T. Prostate carcinomas developing in transgenic rats with SV40 T antigen expression under probasin promoter control are strictly androgen dependent. Cancer Res. **61**: 4693–4700. 2001. [Medline]
22. Sato S, Suzuki S, Naiki-Ito A, Komiya M, Ne L, Kato H, Sagawa H, Yamashita Y, Shirai T, and Takahashi S. Establishment of an invasive prostate cancer model in transgenic rats by intermittent testosterone administration. J Toxicol Pathol. **27**: 43–49. 2014. [Medline] [CrossRef]
23. Naiki T, Asamoto M, Toyoda-Hokaiwado N, Naiki-Ito A, Tozawa K, Kohri K, Takahashi S, and Shirai T. Organ specific Gst-pi expression of the metastatic androgen independent prostate cancer cells in nude mice. Prostate. **72**: 533–541. 2012. [Medline] [CrossRef]
24. Jackson RS 2nd, Franco OE, and Bhowmick NA. Gene targeting to the stroma of the prostate and bone. Differentiation. **76**: 606–623. 2008. [Medline] [CrossRef]
25. Strand DW, Franco OE, Basanta D, Anderson AR, and Hayward SW. Perspectives on tissue interactions in development and disease. Curr Mol Med. **10**: 95–112. 2010. [Medline] [CrossRef]